# Synthesis and Mechanial Properties of Bulk Amorphous Zr-Al-Ni-Cu Alloys Containing ZrC Particles

*Materials Transactions, JIM*, Vol. 38, No. 9 (1997), pp. 793 to 800

# Synthesis and Mechanical Properties of Bulk Amorphous Zr-Al-Ni-Cu Alloys Containing ZrC Particles

Hidemi Kato† and Akihisa Inoue

*Institute for Materials Research, Tohoku University, Sendai 980-77, Japan*

Bulk amorphous $Zr_{55}Al_{10}Ni_5Cu_{30}$ composites containing ZrC particles up to 17 vol% were formed in a cylindrical form with diameters of 1 to 3 mm by a copper mold casting process. The average particle size and interparticle spacing of the ZrC particles are 3 and 4 μm, respectively, and neither distinct agglomeration nor segregation of the ZrC particles is seen on the transverse and longitudinal cross-sections. The glass transition temperature ($T_g$), crystallization temperature ($T_x$) and melting temperature ($T_m$) of the amorphous matrix remain unchanged in the volume fraction ($V_f$) range up to 17%. Neither appreciable second crystalline phase nor voids are seen even at the interface between the amorphous and ZrC phases, though the amorphous matrix has a relaxed disordered structure. The interface has a rugged morphology on a nanometer scale and does not have any faceted plane. The Young's modulus, compressive strength ($\sigma_f$) and Vickers hardness for the composite alloys increase almost linearly from 103 to 125 GPa and 1820 to 2170 MPa and 488 to 563, respectively, with increasing $V_f$ from 0 to 17%. The plastic elongation ($\varepsilon_p$) also increases from nearly zero % at 0 vol% to 0.5% at 10 vol%. The significant increase in $\varepsilon_p$ is presumably due to the increase in the amount of shear sliding before adiabatic final rupture resulting from the increase in $\sigma_f$. The viscous flow of the supercooled liquid is also suppressed by the dispersion of the ZrC particles. The success in synthesizing the high-strength bulk composite alloys consisting of ZrC particles embedded in the amorphous matrix is important for future development of bulk amorphous alloys.

(Received June 4, 1997)

*Keywords*: *bulk amorphous alloy composite, composite material, zirconium carbide, copper mold casting, large glass-forming ability, ceramic dispersion particle, dispersion strengthening, mixture rule*

## I. Introduction

It has recently been reported[1)-3)] that Zr-based amorphous alloys in a multicomponent Zr-Al-Ni-Cu system exhibit a large glass-forming ability and a wide supercooled liquid region. The largest sample thickness for glass formation reaches as large as 30 mm[4)] and the temperature interval of the supercooled liquid region defined by the difference between glass transition temperature ($T_g$) and crystallization temperature ($T_x$), $\Delta T_x(=T_x-T_g)$ is about 127 K[3)]. Besides, the critical cooling rate of the Zr-based amorphous alloys has been measured to be 1 to 5 K/s[5)] from the change in solidification temperature with cooling rate, 10 to 20 K/s[6)] from the continuous cooling curve of the molten alloy on a copper hearth in an arc furnace and about 40 K/s[7)] from the moving velocity and temperature gradient at the liquid/solid interface in the unidirectional solidification mode. The difference in the critical cooling rates has been thought to reflect the difference in the ease of heterogeneous nucleation in their measurement methods.

As one of the methods of improving further mechanical properties of amorphous alloys, it has previously been reported[8)] that the mixture of WC particles in Ni-Si-B amorphous ribbons is effective in the case where the particles disperse homogeneously in the matrix phase and have a good wettability against the matrix phase. When ceramic particles are dispersed in a cast amorphous phase, there is a high risk of generating partial crystallization at the interface between amorphous and ceramic phases. Consequently, there has been no datum on the fabrication and mechanical properties of cast bulk amorphous alloys containing ceramic particles. More recently, it has been found that the use of the Zr-Al-Ni-Cu amorphous alloys with large glass-forming ability enables the fabrication of cast bulk amorphous phase containing homogeneously ZrC particles in the volume fraction range up to 17% and the dispersion of ZrC particle in the absence of any crystalline phase at the interface causes further increases in Young's modulus, compressive fracture strength, compressive plastic elongation and hardness. The first aim of this paper is to present the synthesis of bulk amorphous $Zr_{55}Al_{10}Ni_5Cu_{30}$ alloys containing ZrC particle in the volume fraction range up to 17% by a copper mold casting method and the microstructure, thermal stability and mechanical properties of the bulk amorphous composites. The second is to investigate the effect of the additional ZrC particles on the formation, thermal stability and mechanical properties of the cast Zr-based bulk amorphous alloys.

## II. Experimental Procedure

A quaternary $Zr_{55}Al_{10}Ni_5Cu_{30}$ alloy was examined for the present alloy because it had good ductility even for the bulk amorphous state with a diameter of 30 mm[4)]. The ZrC particle with a diameter of about 3 μm was used for a dispersion medium because of nearly the same specific density as that for the Zr-Al-Ni-Cu alloy. The

† Graduate Student, Tohoku University.

master ingot was prepared by arc melting the mixture of pure Zr, Al, Ni and Cu metals in an argon atmosphere. Subsequently, mixtures of the master Zr-Al-Ni-Cu ingot and various volume fractions of ZrC particles were melted in an argon atmosphere with a high-frequency furnace and cast into copper molds with diameters of 1 and 3 mm and a length of 50 mm. Structure of the composite materials was examined by X-ray diffractometry and optical and transmission electron microscopy (OM and TEM). The apparent specific heat associated with structural relaxation, glass transition, supercooled liquid region and crystallization of the amorphous matrix was measured with a differential scanning calorimeter (DSC) at a heating rate of 0.67 K/s. The melting temperature was also measured with a differential thermal analyzer (DTA) at a heating rate of 0.17 K/s. The values of Young's modulus, compressive strength and plastic elongation were measured at room temperature with an Instron-type testing machine. Elongation was evaluated by a strain gauge meter. The viscosity was measured with a thermal mechanical analyzer at a heating rate of 0.3 K/s.

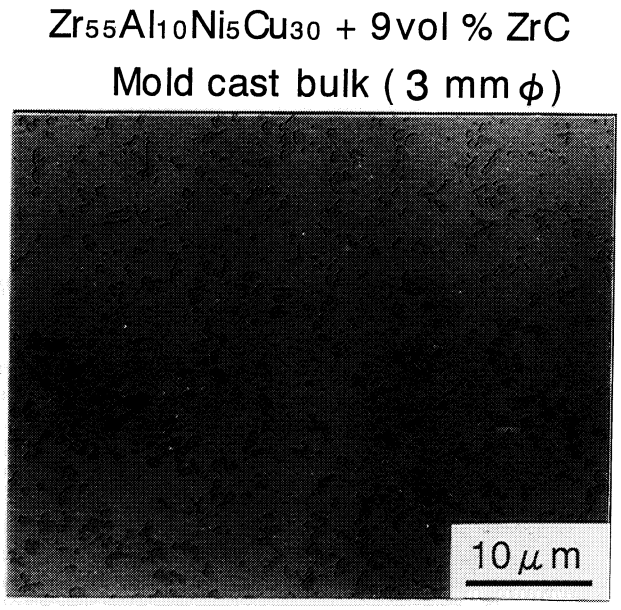


Fig. 1 Optical micrograph of the transverse cross section of a cylindrical bulk $Zr_{55}Al_{10}Ni_5Cu_{30}$ alloy containing 9 vol%ZrC prepared by copper mold casting. The cylinder has a diameter of 3 mm and a length of 50 mm.

## III. Results

### 1. Formation of bulk amorphous and fcc-ZrC composite alloys

Figure 1 shows an optical micrograph of the transverse cross-section for the cast $Zr_{55}Al_{10}Ni_5Cu_{30}$ alloy of 3 mm diameter containing 9 vol%ZrC. It is seen that the ZrC particles with a particle size of about 3 μm are dispersed homogeneously in a matrix phase. The average interparticle spacing is measured to be about 4 μm. Furthermore, neither pore nor void is seen over the whole micrograph, indicating that the amorphous matrix alloy has a good castability. The good castability is attributed to the continuous decreases in the specific volume and the dissoluble amount of gas elements for the amorphous matrix resulting from the absence of the transition from liquidus to crystalline phase. The present copper mold casting method is useful for the synthesis of the composite alloy in which the fine ZrC particles disperse homogeneously. Subsequently, we examined the formation of an amorphous phase in the matrix. Figure 2 shows an X-ray diffraction pattern of the cast $Zr_{55}Al_{10}Ni_5Cu_{30}$ alloy of 3 mm in diameter containing 17 vol%ZrC, together with the data of the $Zr_{55}Al_{10}Ni_5Cu_{30}$ alloy and the ZrC itself. As is evident from comparison with the Zr-Al-Ni-Cu and ZrC phases, the cast bulk alloy consists of amorphous and fcc-ZrC phases and does not contain any other crystalline phase.

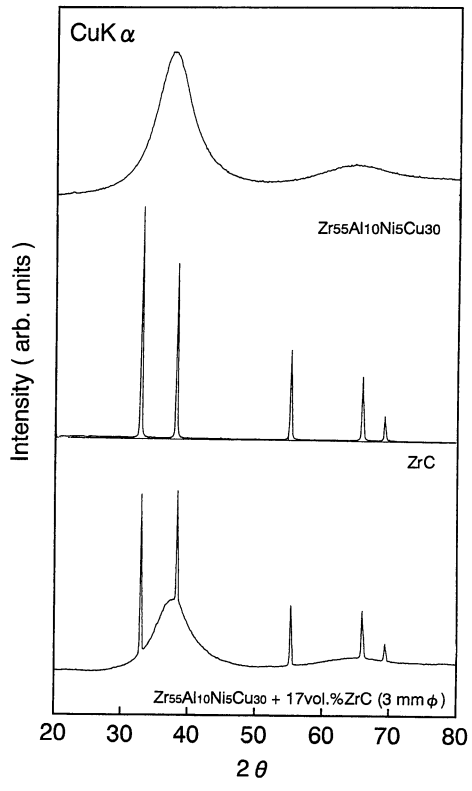


Fig. 2 X-ray diffraction patterns taken from the transverse cross section of a cylindrical bulk $Zr_{55}Al_{10}Ni_5Cu_{30}$ alloy (3 mm$^{\phi}$ × 50 mm) containing 17 vol%ZrC prepared by copper mold casting. The data of cast amorphous $Zr_{55}Al_{10}Ni_5Cu_{30}$ alloy and ZrC particle are also shown for comparison.

Figure 3 shows glass transition temperature ($T_g$), crystallization temperature ($T_x$) and melting temperature ($T_m$) as a function of the volume fraction of ZrC particles ($V_f$) for the bulk amorphous $Zr_{55}Al_{10}Ni_5Cu_{30}$ alloy with a diameter of 3 mm. The $T_g$, $T_x$ and $T_m$ are 683, 767 and 1100 K, respectively, for the amorphous alloy without ZrC partciles and remain unchanged in the entire $V_f$ range up to 17%. The nearly constant values allow us to conclude that the dispersion of the ZrC particle does not cause an appreciable influence on the thermal stability of the amorphous matrix. The absence of the degradation

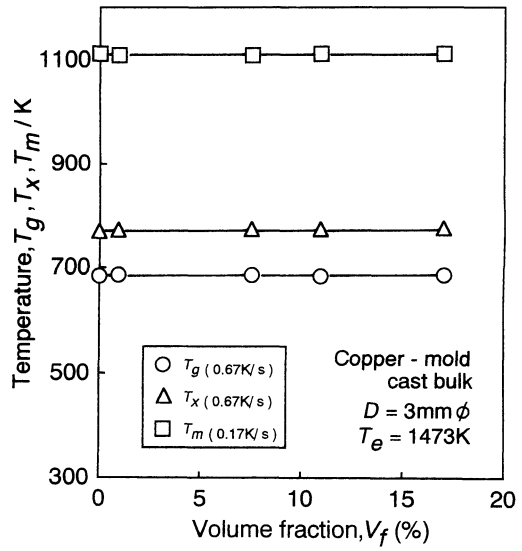


Fig. 3 Changes in the glass transition temperature ($T_g$), crystallization temperature ($T_x$) and melting temperature ($T_m$) with volume fraction of ZrC for the cast bulk amorphous $Zr_{55}Al_{10}Ni_5Cu_{30}$ alloy with a diameter of 3 mm and a length of 50 mm.

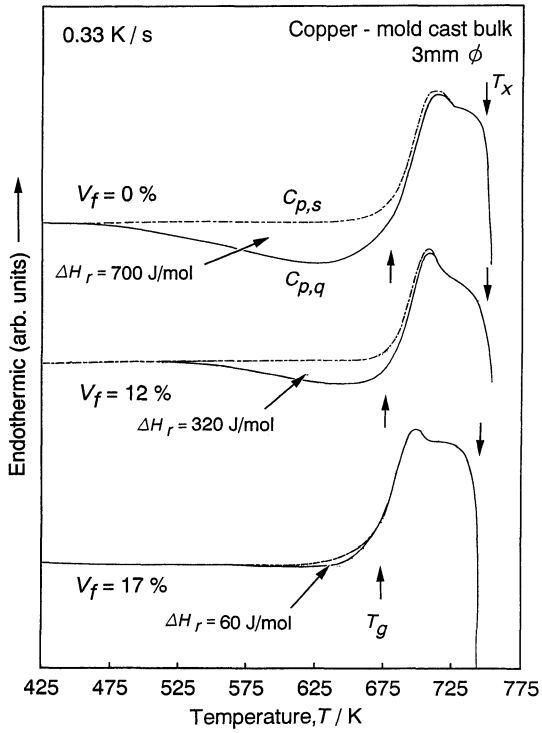


Fig. 4 Thermograms of the cast bulk amorphous $Zr_{55}Al_{10}Ni_5Cu_{30}$ alloys (3 mm$^{\phi}$ × 50 mm) containing 0, 12 and 17 vol%ZrC. The $C_{p,q}$ and $C_{p,s}$ denote the apparent specific heat of the as-cast sample and the sample heated once for 60 s at 710 K, respectively.

of the thermal stability is thought to result from the large glass-forming ability of the Zr-Al-Ni-Cu amorphous alloy. Although no appreciable changes in $T_g$, $T_x$ and $\Delta T_x$ by the dispersion of ZrC particles are seen for the composite materials, the structural relaxation behavior in the temperature range below $T_g$ is expected to change with volume fraction of ZrC particle. Figure 4 shows thermograms of the amorphous $Zr_{55}Al_{10}Ni_5Cu_{30}$ alloys containing ZrC particle ranging from 0 to 17 vol%. The $C_{p,q}$ and $C_{p,s}$ represent the apparent specific heats of the as-cast sample and the sample heated once for 60 s at 710 K, respectively. The difference in the specific heat between the $C_{p,q}$ and $C_{p,s}$ corresponds to the structural relaxation caused by heating. The onset temperature of structural relaxation defined by the deflection point between the $C_{p,q}$ and $C_{p,s}$ curves is measured to be 450 K for the 0 vol% sample, 520 K for the 12 vol% sample and 600 K for the 17 vol% sample. Besides, the heat of structural relaxation defined by $\Delta H_r = \int \Delta C_p (= C_{p,s} - C_{p,q} \geqq 0) dT$ is evaluated to be 700 J/mol for the 0 vol% sample, 320 J/mol for the 12 vol% sample and 60 J/mol for the 17 vol% sample. There is a clear tendency for the degree of structural relaxation to increase with increasing volume fraction of ZrC particle. The formation of the relaxed amorphous structure is presumably because the cooling rate of ZrC particles is much lower than that of the Zr-based amorphous phase and the degradation in cooling capacity of the amorphous matrix by the coexistence of ZrC particles at the lower cooling rate results in the progress of structural relaxation of the amorphous phase which was previously cooled to $T_g$. However, we cannot detect the formation of any crystalline phase in the amorphous phase region just near the interface between the amorphous and ZrC phases. The absence of the crystalline phase is due to the high thermal stability of the amorphous phase against crystallization as well as to the large glass-forming ability of the supercooled liquid.

In order to confirm the absence of any crystalline phase and the achievement of truely bonding state at the interface between amorphous and ZrC phases, transmission electron microscopic observation was made for the composite amorphous and ZrC alloy. Figure 5 shows a bright-field electron micrograph (a) and selected-area electron diffraction patterns (b) to (d) taken from the three different regions of the amorphous matrix, the interface between amorphous and ZrC phases and the ZrC particle, respectively, for the cast bulk amorphous $Zr_{55}Al_{10}Ni_5Cu_{30}$ alloy containing ZrC particle of 17 vol%. The diffraction patterns (b), (c) and (d) can be identified to consist of an amorphous phase, an amorphous plus fcc-ZrC phase and an fcc-ZrC phase, respectively. Even at the interface, no appreciable contrast revealing the precipitation of a crystalline phase is seen in the bright-field image (a), in agreement with the identified result of the electron diffraction pattern (c) taken from the interface region. In addition, neither pores nor voids are observed at the interface in the TEM image. With the aim of examining in more detail the bonding state at the interface, a high-resolution TEM image taken from the interface is shown in Fig. 6. One can clearly see an interfacial structure without pore and void between the amorphous phase with the featureless modulated contrast and the fcc-ZrC phase with the periodic fringe contrast. However, the interface does not lie on a particularly low indexed plane. Furthermore, the interface has a rugged morphology and does not have any faceted plane. The ab-

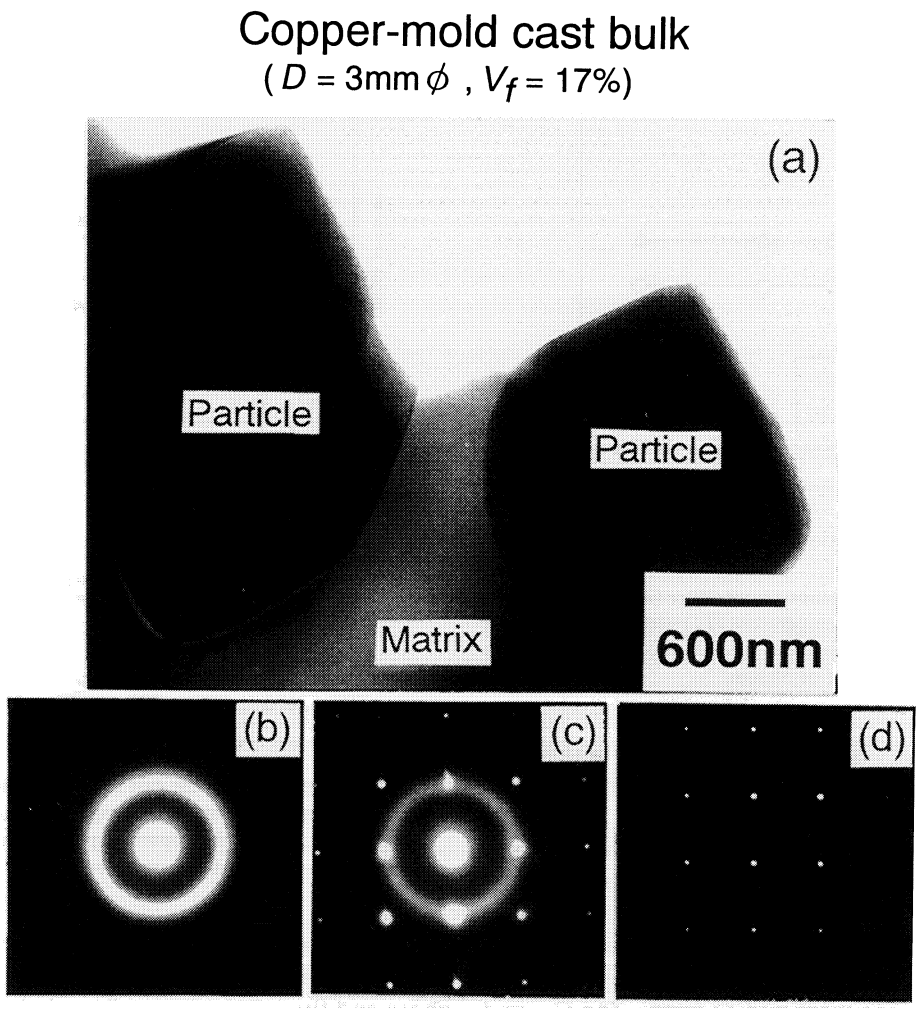


Fig. 5 Bright-field electron micrograph (a) and selected-area electron diffraction patterns (b) to (d) of the cast bulk amorphous $Zr_{55}Al_{10}Ni_5Cu_{30}$ alloy (3 $mm^{\phi} \times 50$ mm) containing 17 vol%ZrC. The (b), (c) and (d) were taken from the matrix region, the interface region between the matrix and particle, and the particle itself, respectively.

sence of a low-indexed facet plane is presumably because the coexistent phase with ZrC phase has a disordered atomic configuration and there is no preferential crystal orientation with a low interface energy. The formation of the well-developed rugged interface on a nanometer scale suggests that the propagation of the crack along the interface is not easy and requires a larger amount of energy as compared with the faceted interface. Besides, neither voids nor other crystalline phase is seen even on a subnanoscale at the interface.

## 2. Mechanical properties and fracture behavior

The homogeneous dispersion of ZrC particle with a particle size of about 3 μm as well as the absence of any crystalline phase at the interface between the amorphous and ZrC phases allows us to expect an increase in mechanical strength. Figure 7 shows changes in the Young's modulus ($E$) and Vickers hardness ($H_v$) with $V_f$ for the cast bulk composite alloy. The $E$ and $H_v$ values are 103 GPa and 488, respectively, at 0 vol%, increase almost linearly with increasing $V_f$ and reach 125 GPa and 563, respectively, at 17 vol%. The dispersion of ZrC particle in the amorphous matrix is effective for the increases in $E$ and $H_v$. Figure 8 shows compressive fracture strength ($\sigma_f$) and plastic elongation ($\varepsilon_p$) as a function of $V_f$ for the composite alloys. The $\sigma_f$ and $\varepsilon_p$ are 1820 MPa and 0.025%, respectively, at 0 vol%, increase significantly with increasing $V_f$ and reach 2170 MPa and 0.5%, respectively, at 10 vol%. It is to be noticed that the $\varepsilon_p$ also increases by the dispersion of ZrC, in addition to the increases in $\sigma_f$, $E$ and $H_v$ values. As examples, Fig. 9 shows a compressive stress-elongation curve of the bulk composite alloy containing 10 vol%ZrC, together with the data on the bulk Zr–Al–Ni–Cu amorphous alloy. It is clearly seen that the composite alloy exhibits higher values of $E$, $H_v$, $\sigma_f$ and $\varepsilon_p$ as compared with those for the amorphous alloy without ZrC. It is particularly notable that the dispersion of 10 vol%ZrC particles increases plastic elongation and $\sigma_f$. Although the increases in $E$, $H_v$ and $\sigma_f$ of the composite alloy by the dispersion of ceramic particles have generally been recognized, this is believed to be the evidence for the increase in $\varepsilon_p$ by the dispersion of ceramic ZrC particles.

In order to investigate the reason for the increase in $\varepsilon_p$ for the composite alloy, compressive fracture behavior and fracture surface appearance for the bulk amorphous

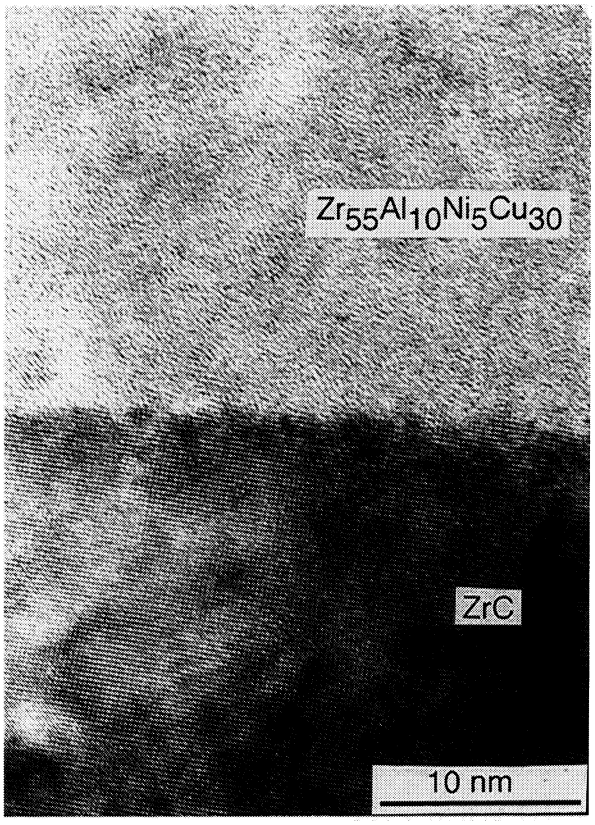


Fig. 6 High-resolution transmission electron micrograph of the interface region between the amorphous and ZrC phases in the cast bulk amorphous $Zr_{55}Al_{10}Ni_5Cu_{30}$ alloy (3 mm$^{\phi}$ × 50 mm) containing 17 vol%ZrC.

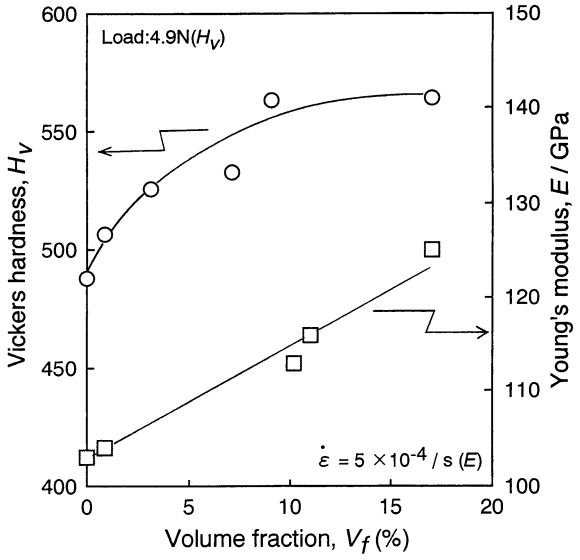


Fig. 7 Changes in the Young's modulus ($E$) and Vickers hardness ($H_v$) with volume fraction of ZrC for the cast bulk amorphous $Zr_{55}Al_{10}Ni_5Cu_{30}$ alloy with a diameter of 3 mm and a length of 50 mm.

Zr-Al-Ni-Cu alloys with 0 vol% and 10 vol%ZrC are shown in Fig. 10. The compressive fracture takes place along the maximum shear plane which is declined by about 45 degrees to the direction of compressive load and

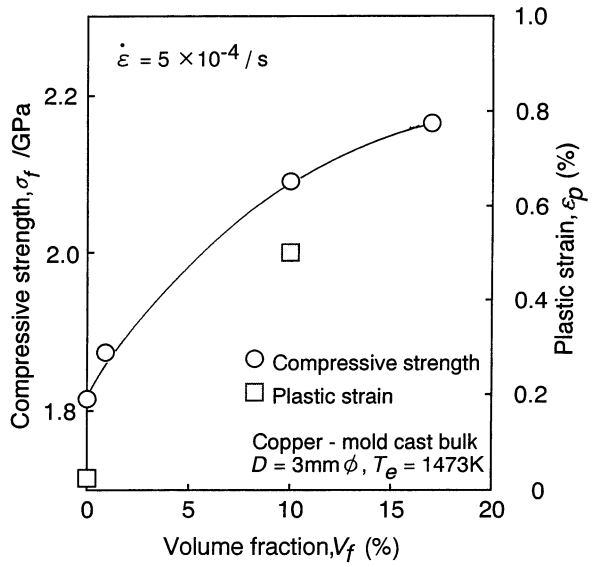


Fig. 8 Change in the compressive strength ($\sigma_f$) with volume fraction of ZrC for the cast amorphous $Zr_{55}Al_{10}Ni_5Cu_{30}$ alloy with a diameter of 3 mm and a length of 50 mm.

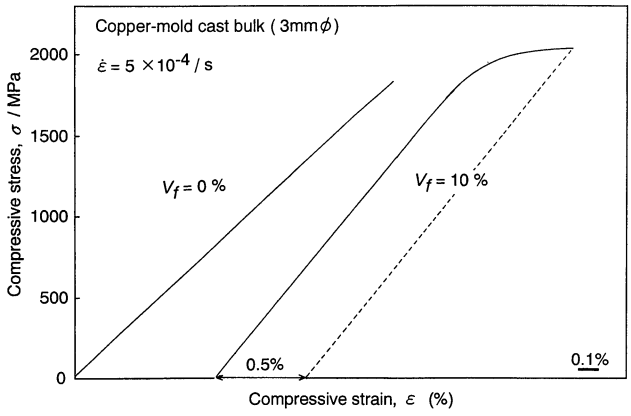


Fig. 9 Compressive stress-elongation curves of the cast bulk amorphous $Zr_{55}Al_{10}Ni_5Cu_{30}$ alloys (3 mm$^{\phi}$ × 50 mm) containing 0 and 10 vol%ZrC.

no distinct difference in the fracture mode is seen between both alloys. Besides, the fracture surface consists of a well-developed vein pattern for both alloys. However, the vein pattern is much finer for the 10 vol% ZrC composite alloy and the movement of the veins appears to be suppressed by ZrC particle. It is known[9] that the fracture of the amorphous alloy takes place by inhomogeneous shear sliding accompanying the generation of a smooth region on the fracture surface, followed by an adiabatic failure at the applied stress level which agrees with the fracture load at the reduced cross section caused by the shear sliding. In general, amorphous alloys have good ductility and can be deformed significantly in the triaxial compressive stress condition even at room temperature[10][11]. For instance, amorphous alloy wires can be cold drawn up to 90% reduction of cross-sectional area without any intermediate annealing treatment[11]-[13]. However, when an amorphous alloy is deformed in an

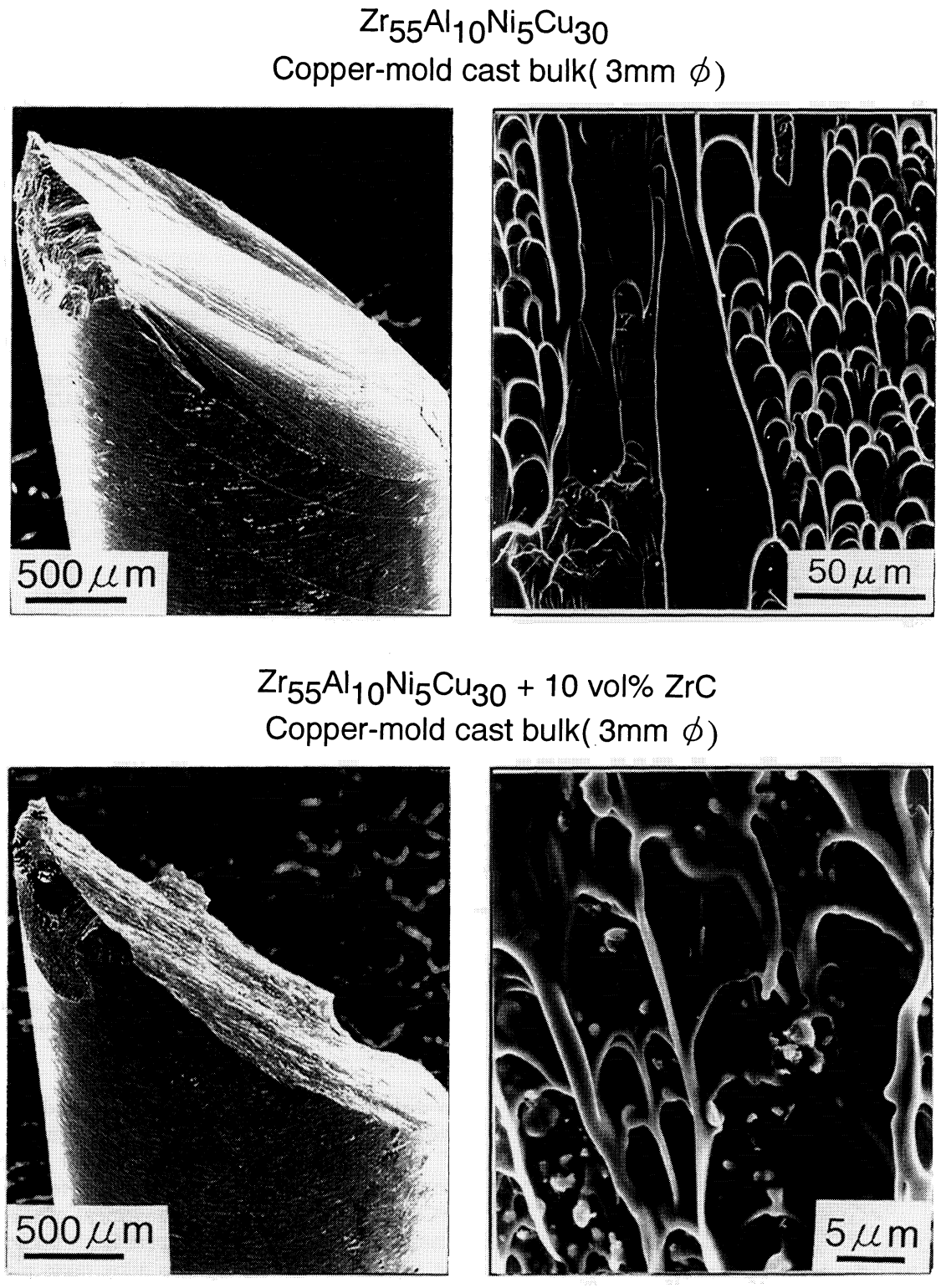


Fig. 10 Compressive fracture behavior and fracture surface appearance of the cast bulk amorphous $Zr_{55}Al_{10}Ni_5Cu_{30}$ alloys containing 0 and 10 vol%ZrC.

uniaxial stress condition, no distinct plastic elongation is obtained because of the absence of strain-hardening ability. It is therefore expected that the endowment of strain-hardening ability causes the appearance of plastic elongation even for the amorphous alloys which are deformed under a uniaxial stress condition. The appearance of plastic elongation resulting from the strain-hardening ability has been thought[14] to occur by the continuous propagation of the inhomogeneous shear sliding along the maximum shear planes. Consequently, if the present elongation for the composite alloy takes place by the same mechanism, the trace of shear sliding is expected to be observed on the lateral outer surface near the fracture site. However, as shown in Fig. 10, no appreciable difference

in the slip markings on the lateral surface near the fracture site is seen between the bulk amorphous alloy without the ZrC phase and the bulk composite alloy consisting of amorphous and ZrC phases. The absence of the distinct slip markings for the bulk composite alloy indicates the existence of the other mechanism for the increase in the plastic elongation. The increase in the compressive elongation is presumably because of the increase in the amount of shear sliding for the amorphous matrix before the final fracture owing to the increase in the final adiabatic fracture load resulting from the increase in the fracture strength for the composite alloy.

### 3. Viscosity of supercooled liquid

It is of importance to clarify the influence of the dispersed ZrC particle on the viscosity of the supercooled liquid. The success of synthesizing the composite alloy consisting of amorphous and ZrC phases in the absence of the other crystalline phase gives a unique opportunity to clarify the viscous flow behavior of the composite amorphous material. Figure 11 shows changes in the minimum viscosity ($\eta_{min}$) of the supercooled liquid and the temperature leading to the minimum viscosity as a function of $V_f$ for the composite alloys. The $\eta_{min}$ value increases almost linearly from $5.8 \times 10^9$ to $131.5 \times 10^9$ Pa·s with increasing $V_f$ from 0 to 17%, while the temperature at which the viscosity reaches the minimum value decreases significantly from 766 to 746 K. These changes indicate that the dispersed ZrC particles can suppress the viscous flow of the supercooled liquid and the viscous flow around the ZrC particles causes the increase in temperature in the local supercooled liquid region just near the interface. The suppression of viscous flow by the dispersion of ZrC particles also implies that the ZrC particle is effective for the increase in the elevated-temperature strength for the bulk amorphous alloys.

## IV. Discussion

It was shown in Figs. 7 and 8 that the dispersion of ZrC particle with a particle size of about 3 μm in the Zr-Al-Cu-Ni amorphous matrix caused the increases in $E$, $\sigma_f$ and $H_v$ as compared with those for the bulk amorphous Zr-based alloy. The interparticle spacing of the ZrC particle was measured to be about 4 μm at 17 vol%. The increase in the mechanical strength is expected to be explained by the simple mixture rule. Since the $E$ and $H_v$ of the ZrC phase itself have been reported to be 390 GPa[15] and 3200[16], respectively, we obtained the predicted $E$ and $H_v$ values of the mixed amorphous and ZrC phases as a function of $V_f$. As shown in Fig. 12, the experimental $H_v$ values lie at the lower side as compared with the values predicted from the mixture rule. The similar tendency is also recognized for $E$, as shown in Fig. 13. The deviation to the lower values for the experimental $H_v$ data is presumed to result from the inhomogeneous deformation mode for the bulk amorphous alloy. It has been reported[17][18] that the inhomogeneous deformation of an amorphous alloy takes place through massive movement of the constituent atoms within a local region with a thickness of about 10 to 20 nm. On the other hand, the interparticle spacing of the ZrC particles is 4 μm which is about 200 to 400 times larger than the thickness of the shear deformation band. The significant difference implies the possibility that the amorphous alloy containing the ZrC particls can be deformed only in the amorphous phase region and the dispersed ZrC particle does not affect the deformation behavior.

However, the $E$ values which do not include any con-

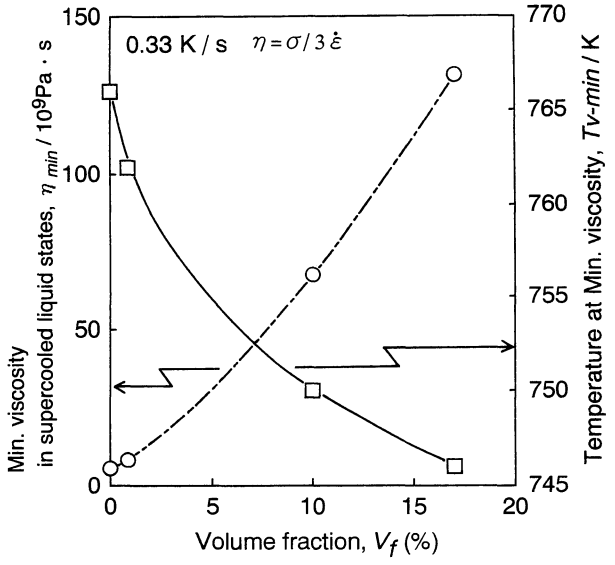


Fig. 11 Changes in the minimum value of viscosity of the supercooled liquid ($\eta_{min}$) and the temperature at which the viscosity is minimum ($T_{\eta,min}$) as a function of volume fraction of ZrC for the cast bulk amorphous $Zr_{55}Al_{10}Ni_5Cu_{30}$ alloys with a diameter of 3 mm and a length of 50 mm.

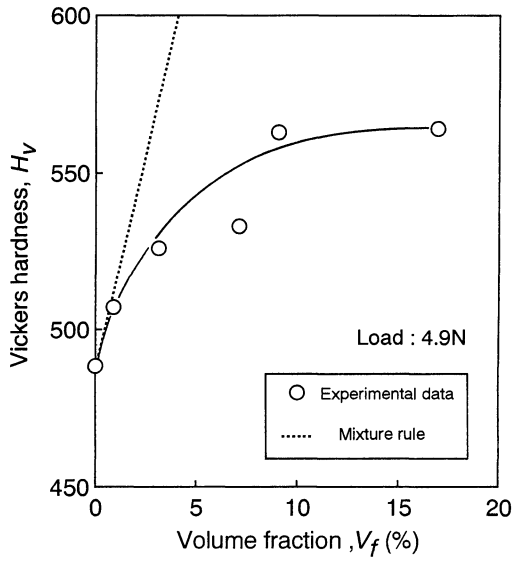


Fig. 12 Vickers hardness ($H_v$) as a function of volume fraction of ZrC for the cast bulk amorphous $Zr_{55}Al_{10}Ni_5Cu_{30}$ alloys with a diameter of 3 mm and a length of 50 mm. The data expected from the mixture rule are also shown for comparison.

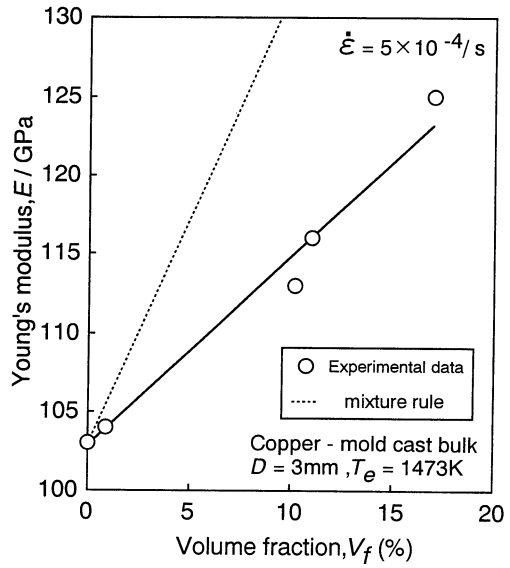


Fig. 13 Young's modulus ($E$) as a function of volume fraction of ZrC for the cast bulk amorphous $Zr_{55}Al_{10}Ni_5Cu_{30}$ alloys with a diameter of 3 mm and a length of 50 mm. The data expected from the mixture rule are also shown for comparison.

tribution to plastic deformation also deviate to the lower side from the mixture rule. The deviation in the $E$ value is presumably due to a weak bonding nature without any coherent relation between fcc ZrC and amorphous Zr–Al–Ni–Cu phases. The ZrC/amorphous interface has a lower interfacial energy as compared with that for solid/solid interfacial energy. However, the interface does not have any crystallographic coherency and the absence of the coherent relation at the interface between ZrC/amorphous phase causes the weakness of the bonding nature between the two phases, leading to the negative deviation of $E$ to the mixture rule. Besides, one can see the difference in the changes in $E$ and $H_v$ as a function of $V_f$, as shown in Figs. 12 and 13. That is, the increase in $E$ is almost linear, while the $H_v$ increases in the $V_f$ range below about 10% and then becomes constant. Considering that structural relaxation proceeds with increasing $V_f$, the nonlinear relation for $H_v$ is presumably because of the decrease in the deformability under a severe strain field with increasing $V_f$.

## V. Summary

We examined the possibility of fabricating the bulk amorphous $Zr_{55}Al_{10}Ni_5Cu_{30}$ composites containing homogeneously dispersed ZrC particle by a copper mold casting method. The results obtained are summarized as follows.

(1) Bulk amorphous alloys containing up to 17 vol% ZrC were prepared in the diameter range of 1 to 3 mm. The average particle size and interparticle spacing of the ZrC particles are 3 and 4 μm, respectively. Neither appreciable agglomeration nor segregation for the ZrC particle is observed.

(2) No other crystalline phase is seen at the interface between the amorphous and ZrC phases. The interface has a rugged morphology on a nanometer scale and does not have any faceted plane of the ZrC phase.

(3) The $E$, $\sigma_f$ and $H_v$ increase almost linearly from 103 to 125 GPa, 1820 to 2170 MPa and 488 to 563, respectively, with increasing $V_f$ from 0 to 17%. These increases are interpreted by the dispersion strengthening of the ZrC particle. In addition, the $\varepsilon_p$ also increases from nearly zero for the 0 vol% alloy to 0.5% for the 10 vol% alloy. The increase in the plastic elongation is probably due to the increase in the amount of shear sliding before adiabatic final fracture resulting from the increase in fracture strength.

(4) The increase in the maximum value of viscosity in the supercooled liquid region is due to the dispersion of ZrC particle and hence the dispersed particle is also effective for the increase in the elevated temperature strength. The synthesis of the bulk amorphous plus ZrC composites with improved mechanical strength and ductility is encouraging for future development in the basic science and engineering application of bulk amorphous alloys.

*Acknowledgment*

One of the authors (A. Inoue) is grateful to the Grant-in-Aid for Specially Promoted Research of The Ministry of Education, Science, Sports and Culture for support of this research.

REFERENCES

(1) A. Inoue, T. Zhang and T. Masumoto: Mater. Trans., JIM, **31** (1990), 177.
(2) A. Inoue, T. Zhang and T. Masumoto: J. Non-Cryst. Solids, **156–158** (1993), 473.
(3) T. Zhang, A. Inoue and T. Masumoto: Mater. Trans., JIM, **32** (1991), 1005.
(4) A. Inoue and T. Zhang: Mater. Trans., JIM, **37** (1996), 185.
(5) A. Inoue: Mater. Trans., JIM, **36** (1995), 866.
(6) A. Inoue: Sci. Rep. Res. Inst. Tohoku Univ., **A42** (1996), 1.
(7) Y. Yokoyama and A. Inoue: Mater. Trans., JIM, **36** (1995), 1398.
(8) H. Kimura, T. Masumoto and D. G. Ast: Acta Metall., **35** (1987), 1757.
(9) R. Maddin and T. Masumoto: Mater. Sci. Eng., **9** (1972), 153.
(10) S. Takayama: J. Mater. Sci., **11** (1976), 164.
(11) M. Hagiwara, A. Inoue and T. Masumoto: Met. Trans., **13A** (1982), 373.
(12) A. Inoue, M. Hagiwara and T. Masumoto: J. Mater. Sci., **17** (1982), 580.
(13) M. Hagiwara, A. Inoue and T. Masumoto: Mater. Sci. Eng., **54** (1982), 197.
(14) A. Inoue, Y. H. Kim and T. Masumoto: Mater. Trans., JIM, **33** (1992), 487.
(15) V. G. Bukatov, V. I. Knyazev, O. S. Korostin and V. M. Baranov: Izv Akad. Nauk SSSR Neorg. Mater., **11** (1976), 367.
(16) *Metals Databook*, ed. by Japan Inst. Metals, Maruzen, Tokyo (1974), p. 141.
(17) *Materials Science of Amorphous Alloys*, ed. by T. Masumoto, Ohmu Pub., Tokyo (1981), p. 201.
(18) J. C. M. Li: *Rapidly Solidified Alloys*, ed. by H. H. Liebermann, Marcel Dekker, Inc., New York, (1993), p. 379.